The conserved barH-like homeobox-2 gene barhl2 acts downstream of orthodentricle-2 and together with iroquois-3 in establishment of the caudal forebrain signaling center induced by Sonic Hedgehog

Hugo Juraver-Geslin, José Luis Gomez-Skarmeta, Beatrice Claude Durand

Developmental Biology 396 (2014) 107–120

Contents lists available at ScienceDirect

Developmental Biology

journal homepage: www.elsevier.com/locate/developmentalbiology

The conserved barH-like homeobox-2 gene *barhl2* acts downstream of *orthodentricle-2* and together with *iroquois-3* in establishment of the caudal forebrain signaling center induced by Sonic Hedgehog

Hugo A. Juraver-Geslin [a,b,c,d,1], José Luis Gómez-Skarmeta [e], Béatrice C. Durand [a,b,c,d,*]

[a] Ecole Normale Supérieure, Institut de Biologie de l'ENS, IBENS, S1.7 46 rue d'Ulm 75005, Paris F-75005, France
[b] INSERM, U1024, Paris F-75005, France
[c] CNRS, UMR 8197, Paris F-75005, France
[d] S1.7 46 rue d'Ulm, 75005 Paris, France
[e] Centro Andaluz de Biología del Desarrollo-CSIC/Universidad Pablo de Olavide, Carretera de Utrera, Km1, 41013 Sevilla, Spain

ARTICLE INFO

Article history:
Received 23 January 2014
Received in revised form
13 August 2014
Accepted 23 September 2014
Available online 2 October 2014

Keywords:
Development
Forebrain
Morphogenesis
Sonic Hedgehog
Signaling
Compartment

ABSTRACT

In this study, we investigated the gene regulatory network that governs formation of the *Zona limitans intrathalamica* (ZLI), a signaling center that secretes Sonic Hedgehog (Shh) to control the growth and regionalization of the caudal forebrain. Using loss- and gain-of-function, explants and grafting experiments in amphibians, we demonstrate that *barhl2* acts downstream of *otx2* and together with the *iroquois* (*irx*)-3 gene in establishment of the ZLI compartment initiated by Shh influence. We find that the presumptive (pre)-ZLI domain expresses *barhl2, otx2* and *irx3*, whereas the thalamus territory caudally bordering the pre-ZLI expresses *barhl2, otx2* and *irx1/2* and early on *irx3*. We demonstrate that Barhl2 activity is required for determination of the ZLI and thalamus fates and that within the p2 alar plate the ratio of Irx3 to Irx1/2 contributes to ZLI specification and size determination. We show that when continuously exposed to Shh, neuroepithelial cells coexpressing *barhl2*, *otx2* and *irx3* acquire two characteristics of the ZLI compartment—the competence to express *shh* and the ability to segregate from anterior neural plate cells. In contrast, neuroepithelial cells expressing *barhl2, otx2* and *irx1/2*, are not competent to express *shh*. Noteworthy in explants, under Shh influence, ZLI-like cells segregate from thalamic-like cells. Our study establishes that Barhl2 activity plays a key role in p2 alar plate patterning, specifically ZLI formation, and provides new insights on establishment of the signaling center of the caudal forebrain.

Introduction

Vertebrate brain patterning is a highly complex process, involving simultaneous and sequential steps that subdivide a morphologically homogeneous neuroepithelial sheet into distinct neural territories (reviewed in Hoch et al., 2009; Wilson and Houart, 2004). During the early steps of neural induction, an underlying prepattern emerges in the neural plate, partly encoded by transcription factors (TFs). These early patterning cues contribute to the specification of forebrain (diencephalon and telencephalon) territories and influence the way neighboring cell populations respond differentially to similar morphogens (Gomez-Skarmeta et al., 2003; Kobayashi et al., 2002; Robertshaw et al., 2013). Based on the expression patterns of TFs, the diencephalic primordium is divided into three transverse segments called prosomeres (p) that generate three distinct histogenic fields (reviewed in Puelles and Rubenstein, 2003): p3 corresponds to the prethalamus; p2 gives rise to the epithalamus and the thalamus; and p1 generates the presumptive pretectum (reviewed in Figdor and Stern, 1993; Martinez-Ferre and Martinez, 2012; Puelles and Rubenstein, 2003). Each prosomere is divided into a ventral (basal) and a dorsal (alar) part. The patterning, proliferation and morphogenesis of the thalamus (p2) are controlled by morphogenic factors secreted by the *Zona Limitans Intrathalamica* (ZLI), also called Mid-Diencephalic Organizer (MDO) (reviewed in Chatterjee and Li, 2012; Kiecker and Lumsden, 2012; Martinez-Ferre and Martinez, 2012; Scholpp and Lumsden, 2010). The ZLI is defined by the alar plate expression of *shh,* a secreted morphogen that mediates

* Corresponding author. Present address: Team Signaling and Neural Development, Université Paris Sud, Institut Curie, U1021 INSERM, UMR3347 CNRS Institut Curie, Centre de Recherche Centre Universitaire, Batiment 110, F-91405 Orsay Cedex, France.
E-mail address: Beatrice.Durand@curie.fr (B.C. Durand).
[1] Present address: New York University – College of Dentistry, Department of Basic Science & Craniofacial Biology, 345 E. 24th Street, 1005S New York, NY 10010-4086, USA.

http://dx.doi.org/10.1016/j.ydbio.2014.09.027
0012-1606/

regionalization of the prethalamus anteriorly, and the thalamus posteriorly (Hashimoto-Torii et al., 2003; Kiecker and Lumsden, 2004; Scholpp et al., 2006; Vieira et al., 2005). Cell-lineage analysis has demonstrated that the ZLI is a cellular compartment, which is delimited by boundaries anteriorly and posteriorly (Garcia-Lopez et al., 2004; Larsen et al., 2001; Zeltser et al., 2001).

The ZLI develops at the interface between the expression domains of the transcription factor genes *fezf2*, which marks the

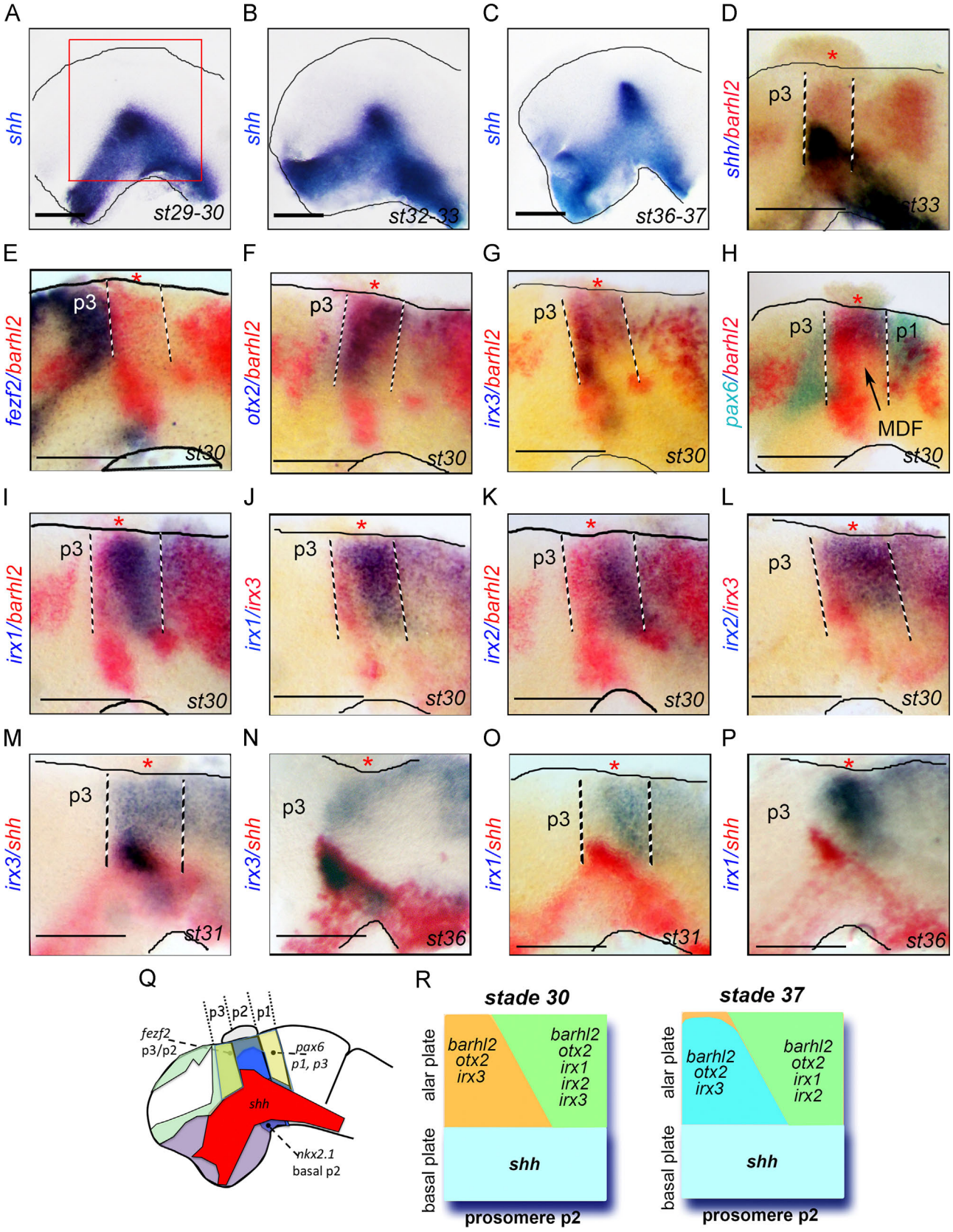

alar plate of p3, and *irx3*, which marks the p2 territory (Martinez-Ferre et al., 2013; Shimamura et al., 1995; Vieira and Martinez, 2006; Zeltser, 2005). In chicken, the *shh*-expressing line of cells corresponding to the ZLI appears through a sequential induction process, initiated by Shh secreted by basal plate cells. Observations in zebrafish and chick highlight early and late roles for Wnt ligands in ZLI induction and development (Martinez-Ferre et al., 2013; Mattes et al., 2012). A current hypothesis holds that diencephalic tissues that lie rostral and caudal to the position of the ZLI are refractory to the Shh-dependent induction of *shh* expression (reviewed in Epstein, 2012; Hagemann and Scholpp, 2012; Martinez-Ferre and Martinez, 2012; Scholpp and Lumsden, 2010). However, identities of the TFs that control ZLI competence to express *shh* and contribute to establish the ZLI compartment identity during development of the caudal forebrain are incompletely understood.

During early neurulation, the *orthodentricle-2* (*otx2*) expression territory marks the anterior neural plate (Pannese et al., 1995). The *iroquois* expression domains—*irx1, irx2, irx3*—mark the caudal forebrain (Rodriguez-Seguel et al., 2009), and the corresponding TFs have all been demonstrated to play a part in ZLI development. In mouse and zebrafish, the ZLI anterior boundary is established through cross-inhibitory interactions between Fezf2 and Irx3 and, at later developmental stages, between Fezf2 and Otx2 (Hirata et al., 2006; Jeong et al., 2007; Rodriguez-Seguel et al., 2009; Scholpp et al., 2007). Depletion of *irx1* orthologs *irx1b/irx7* in zebrafish induces a posterior shift of the ZLI caudal border (Hirata et al., 2006; Scholpp et al., 2007). The presence of Otx1l/2 is required to establish a competence area, allowing induction of *shh* in the ZLI (Hirata et al., 2006; Scholpp et al., 2007). In *Xenopus laevis*, transcripts encoding the barH-like homeobox 2, *barhl2* are detected in the diencephalic primordium from early neurulation onwards, and the ZLI develops within a domain expressing *barhl2* (Juraver-Geslin et al., 2011; Offner et al., 2005). We previously described a pathway controlled by Barhl2 that cell-autonomously limits the amount and/or the activation of the effector of the canonical Wnt pathway, ß-catenin (Juraver-Geslin et al., 2011). However, the functions of Barhl2 in the specification of ZLI identity and properties have not been investigated.

In this study, we investigated establishment of the ZLI territory in *Xenopus laevis* embryos. We established that at the onset of ZLI formation, the expression of *irx* genes subdivides the p2 alar plate histogenic field into two territories and that the ZLI develops within the rostral p2 territory. We demonstrate that in Barhl2-depleted embryos the border between prosomeres p2 and p3 is established properly, whereas formation of the ZLI is abolished and patterning of the thalamus is abnormal. Moreover within the p2 alar plate, changes in the Irx3 to Irx1/2 ratio modify the size of the ZLI territory. Importantly we demonstrate that in explants and in grafted embryos, when continuously exposed to Shh, cells expressing *barhl2*, *otx2* and *irx3* recapitulate the main features of their normal *in vivo* developmental program: cells co-expressing *barhl2*, *otx2* and *irx3* are competent to express *shh* and segregate from cells of other anterior neural lineages, except those expressing thalamus genes i.e. *barhl2*, *otx2*, *irx1* and *irx2*. Moreover, Shh enables the ability of *barhl2*, *otx2*, *irx3* expressing cells to sort-out from cells expressing *barhl2*, *otx2*, *irx1* and *irx2*.

Materials and methods

Embryos and injection

Xenopus embryos were obtained by *in vitro* fertilization and staged according to Nieuwkoop and Faber. Capped RNAs (cRNA) were prepared from pCS2 derivatives (Ambion). Except when otherwise specified, *MObarhl2* (60 ng), *MOirx1* together with *MOirx2* (45 ng of each) were injected, together with *ß-gal* or *gfp* cRNA (100 pg) as tracers, into dorsal blastomere of four-cell stage embryos. cRNA encoding *irx3* (100 pg), ß-catenin MO (10 ng), control MO coupled to fluorescein (*MOct*, 5 ng) and except when specified otherwise, together with a tracer were injected into the dorsal blastomere, D1.1 or D1.2 (Moody, 1987), of eight- or 16-or 32-cell stage embryos. To minimize defects in axial organizer formation anterior parts of the neural tubes were targeted and embryos selected accordingly. For all rescue and overexpression experiments, a range of cRNA doses (50–300 pg) was tested, and the minimal cRNA quantity that induced the phenotype and displayed no toxicity was selected. A phenotype exhibited by at least 70% of the embryos was considered significant. Three independent experiments were performed and the results were pooled.

Antisense morpholinos

Antisense oligonucleotides either with no 5′ capping, either coupled to fluorescein were made by Gene-Tools as previously published: *MObarhl2* (Offner et al., 2005), *MOirx1* and *MOirx2* (Rodriguez-Seguel et al., 2009), *MOßcat* (Heasman et al., 2000) and control MO (*MOct*) coupled to fluorescein (Gene-tools).

Animal cap explants and grafting experiments

Eight-cell stage embryos were injected into the four animal blastomeres with either a cRNA encoding for a secreted form of *shh* from rat N-Shh (50 pg/blastomere; generous gift RJ. Wechsler-Reya), or cRNA encoding for indicated transcription factors (50 pg/blastomere). We injected *noggin* cRNA (50 pg/blastomere) to anteriorize the animal caps (AACs), *gfp* or *ß-gal* cRNA (50 pg/blastomere) as tracers. For sandwiched explants at least 24 ACs were analyzed for each conditions and three independent experiments were performed. For mixed explants at least 8 AACs were

Fig. 1. The ZLI develops inside the rostral alar p2 territory that expresses *barhl2*, *otx2*, *irx3* and does not express *irx1* and *irx2*. ISH or Double ISH on wt embryos, shown as dissected neural tubes from a side view, dorsal up, anterior left. The markers and stages are indicated. (D)–(P) Enlargement views centered on p2 as indicated by the red square on A. The pineal gland (red star) located on top of p2 is used as a morphological landmark. The black dashed lines are indicative of the putative anterior and posterior borders of p2. The scale bar stands for 0.5 mm. p: prosomere; MDF: Mid Diencephalic Furrow. (A–C) Time course analysis of *shh* expression in the *Xenopus* forebrain: (A) at st. 29 and st. 30 *shh* is only expressed in the forebrain floor and basal plates; (B) at st. 32 *shh* is detected in the forming ZLI; (C) at st. 37 development of the ZLI is mostly achieved. (D–L) At st. 30 and st. 31 the p2 alar plate contains two subdomains. (D) The ZLI forms in a domain that expresses *barhl2*. (E) The p2 anterior limit of *barhl2* abuts that of *fezf2*, which marks the p3/p2 boundary; in the p2 alar plate *barhl2* is co-expressed with (F) *otx2* and (G) *irx3*. (H) *pax6* marked p1 and p3 but is excluded from p2, except for the most dorsal part, which gives rise to the epithalamus. *barhl2* is expressed in the part of the p2 domain devoid of *pax6* expression, i.e. the mid-diencephalic furrow. A comparative analysis of *barhl2* and (I–L) *iroquois* expression revealed two subdomains inside the alar p2: a rostral p2 domain that expresses *barhl2* (I, K), *otx2* (F), *irx3* (G, J, L) and a caudal p2 domain that expresses *barhl2* (I, K), *otx2* (F), *irx3* (G, J, L), *irx1* (I, J) and *irx2* (K, L). (M–P) The ZLI develops inside the rostral p2 domain. Double ISH on st. 32 and st. 36 dissected neural tubes with *shh* and *iroquois* genes that mark either the rostral p2 territory (M, N) *irx3*, or the caudal p2 territory (O, P) *irx1* as probes. The alar progression of *shh* expression occurs in a domain that expresses *irx3* (M, N) but not *irx1* (O, P). (Q) Schematic of diencephalic markers at st. 31. Prosomere p2 is indicated in blue; Areas of expression are shown for *fezf2* (green) a marker of the p3–p2 border; *nkx2.1* (purple) that marks basal p2; *shh* (red) marks the p2 basal plate and the ZLI; p1, p3 and the epithalamus are revealed using *pax6* (yellow). (R) Schematic of dynamics of p2 alar plate markers expression: The basal plate expresses *shh* (light blue). Within the p2 territory devoid of *pax6* but expressing *barhl2* and *otx2:* At stage 30 the rostral domain expresses *irx3* and not *irx1/2* (orange) the caudal domain expresses *irx1/2/3* (green). At stage 37 the rostral domain expressed the same markers and *shh* (light blue) and the caudal domain expresses *irx1/2* (green).

pooled and two independent experiments were performed. Cells were dissociated in PBS Ca^{2+}-free and Mg^{2+}-free with BSA (0.2%). The pigmented epithelium was removed manually. Once dissociated, cells of AACs of each conditions were pooled, centrifugated at low speed for 30 s, resuspended in 0.5XMMR with gentamycin, and let to re-associate for at least 3 h at 18 °C. Both type of AACs were let to develop until their siblings had reached st. 32. For sectioning, explants were embedded in Albumin/Gelatin mix for vibratome sectioning (40 μm). For grafting, mixed explants were generated and let to develop until their siblings had reached st. 14. A piece of mixed explant was carefully rinsed and immediately put in a longitudinal or lateral incisions within the neural plate of a st. 14 embryo. Operated embryos were then grown until stages 35.

Whole mount in situ hybridization (ISH)

Double and single ISH were performed using digoxigenin-labeled or fluorescein-labeled probes as previously described (Harland, 1991; Turner and Weintraub, 1994). The ectoderm overlying the anterior neural tube together with the eyes was removed before ISH. In the cases where the presence of a MO-coupled to fluorescein (co-injection with *MOßcat*) was revealed, the digoxigenin-labeled probe was first detected with BM-purple, followed by revelation of the fluorescein with Fast Red (Roche) according to the manufacturer's instructions. The neural tubes of chosen specimens were dissected in PBS-Tween 0.1% and stored in 90% glycerol. For flat-mounted embryos, the neural tubes were bisected along the dorsal and ventral midlines with a tungsten needle and mounted in 90% glycerol. The same settings were used for images acquisition of both the control and the injected sides of whole mount ISH of each dissected neural tube to allow direct comparison. The dissected neural tubes are always shown side view, anterior left, dorsal up.

X-gal staining

Embryos were fixed in paraformaldehyde 4% for 30 min, washed in phosphate buffer, and transferred into Red-Gal (Research Organics) staining solution (Coffman et al., 1990).

Preparation of Shh-N containing medium and beads

HEK 293T cells, cultured in DMEM 10% Fetal Calf Serum (Gibco), were trypsinized and seeded on 10 cm Petri dishes. Calcium phosphate transfection of the Shh-N or the pcDNA3 plasmids was performed. The supernatant from every consecutive day was pooled and filtered through a 0.45 μm filter. N-Shh was neutralized through overnight pre-incubation with serum containing the monoclonal antibody 5E1 (Ericson et al., 1996). Before being placed onto the AAC, anion exchange resin beads (Biorad #140-1231) were rinsed in distilled water five times, soaked in a BSA solution and incubated for at least 2 h in the N-Shh conditioned medium, in the presence or absence of the neutralizing 5E1 antibody. At least 30 AACs were analyzed for each experimental condition and two independent experiments were performed.

Pharmacological treatments

Inducible Irx3 (Irx3-GR) was activated by dexamethasone (Kolm and Sive, 1995).

Results

The expression of irx genes during ZLI development subdivides the p2 alar plate histogenic field

The alar part of diencephalic p2 generates the thalamus and the ZLI (reviewed in Martinez-Ferre and Martinez, 2012; Puelles and Rubenstein, 2003). A schematic diagram of gene expression territories of the developing amphibian diencephalon is provided in Fig. 1Q. We investigated the dynamics of *shh* expression within the forming ZLI in *Xenopus laevis* embryos from st. 29–37. We observed that the expression starts at st. 30 and increases until st. 37 (Fig. 1A–C). We delimited the alar/basal plate boundary of the diencephalon at the base of the ZLI area that coincides with the limit of *shh* intense staining. In agreement with observations in chick embryos (Zeltser, 2005), at st. 37 *shh* expression had extended to 70% of the alar plate length. We previously observed that the ZLI develops within a territory that expresses *barhl2* (Juraver-Geslin et al., 2011) (Fig. 1D). We now investigated the expression patterns of *barhl2*, compared to markers of the p2-p3 border and of the p2 alar plate, before and during ZLI development.

Whereas at st. 27 *barhl2* is a specific marker of p2, at st. 31 the *barhl2* expression domain diversified: it was expressed in the cortical hem, p2 and the midbrain (Juraver-Geslin et al., 2011). Before ZLI development, the p2 anterior border of *barhl2* expression abuts the caudal border of *fezf2* expression in p3 (Fig. 1E). In the alar plate, *barhl2* expression overlaps with that of *otx2* (Fig. 1F) and *irx3* (Fig. 1G). Double *in situ* hybridization (ISH) with *pax6* indicated that *barhl2* was expressed in the part of the p2 domain devoid of *pax6* expression which is referred to as the mid-diencephalic furrow (Fig. 1H). We compared the expression of *barhl2* with that of the *iroquois* genes that mark the diencephalic primordium from early neurulation onwards (Rodriguez-Seguel et al., 2009), and play a role in delimitating the anterior and posterior borders of the ZLI. We observed that at st. 30 and st. 31 *irx3* is expressed in the entire alar p2 domain (Fig. 1G), whereas *irx1* and *irx2* are excluded from the rostral part of the p2 alar plate (Fig. 1I–L).

We compared expression of the ZLI marker *shh* with markers of rostral p2 and caudal p2 at st. 31 and st. 36, after the ZLI started to form. We observed that the progression of *shh* expression into the p2 alar plate was restricted to the rostral p2 territory (Fig. 1M–P). With time, the alar progression of the ZLI was concomitant with a shift of *irx3* expression territory to the rostral p2. At the same developmental stages, *irx1* and *irx2* expression domains were restricted to caudal p2 (Fig. 1M–P).

Thus, in *Xenopus laevis* embryos, the alar p2 domain that expresses *barhl2* and *otx2* and is devoid of *pax6* encompasses two territories: rostral p2, which expresses *irx3* but not *irx1/2*, and caudal p2, which at st. 30 expresses *irx1/2/3* and after st. 37 expresses only *irx1/2* (Fig. 1R). The ZLI develops within the rostral p2 territory.

Barhl2 depletion impairs the establishment of the p2 alar plate territories

Zebrafish embryos that are deficient in both *otx1l* and *otx2* expression exhibit a loss in *barhl2* expression and have ZLI developmental defects (Scholpp et al., 2007). Using a previously characterized MO against *barhl2* (*MObarhl2*) (Offner et al., 2005), we examined the effects of Barhl2-depletion on the establishment of the p2 alar plate.

Upon inhibition of Barhl2 activity, no changes were detected in the expression of *fezf2*, *arx2* and *emx2*, which marked the p3–p2 prosomeric limit (Fig. 2A, B; Fig. S1). The expression domains of *nkx2.1* (ventral p2), *otx2* (p2), and the Wnt-pathway TF gene *tcf4* (p2 and p1), were unaffected (Fig. 2C–E). Therefore, p2 cells are present and partly specified in these embryos. The patterning of

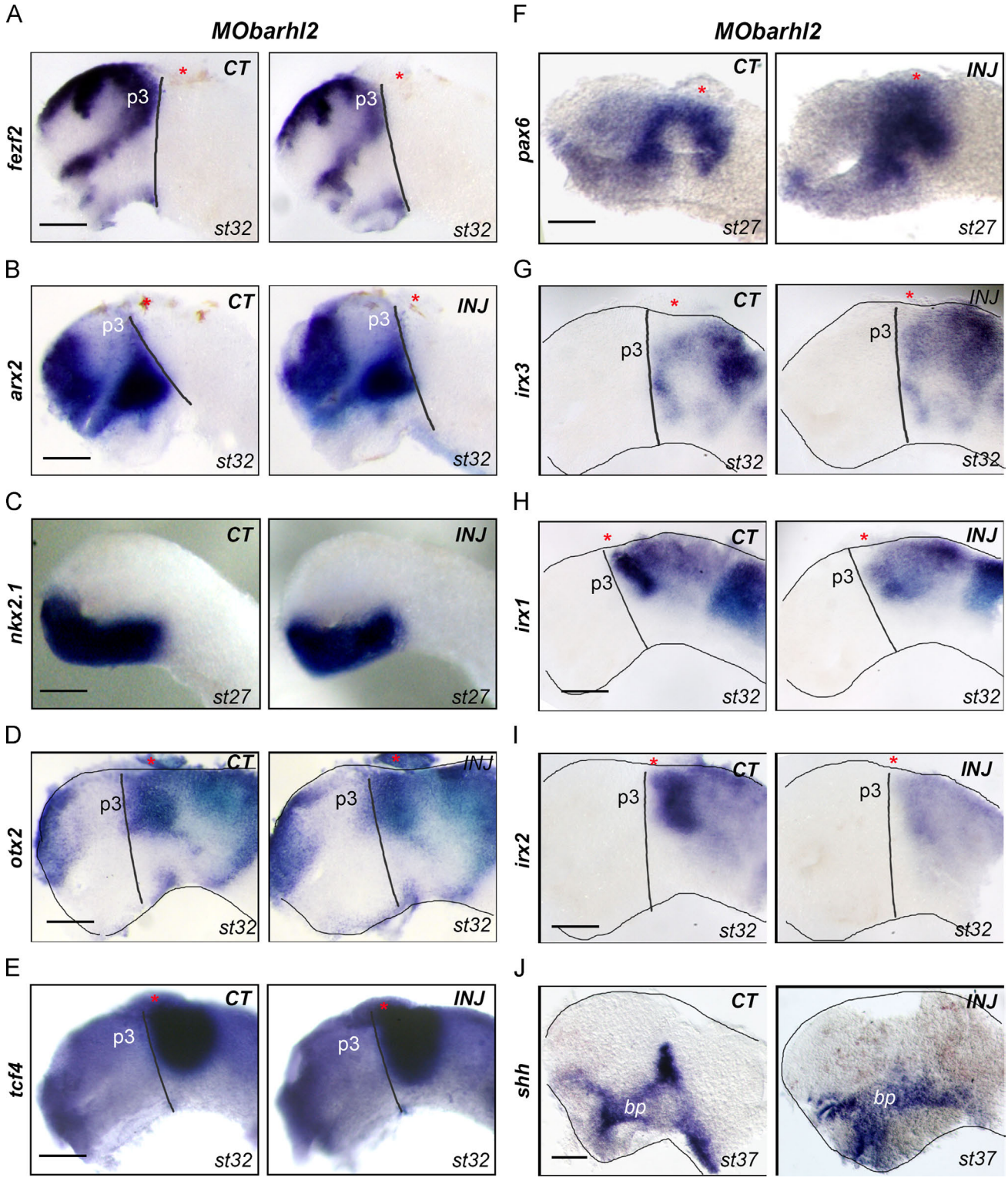

Fig. 2. Barhl2-depleted embryos exhibit defects in p2 alar plate patterning. Gene expression profiles of forebrain markers in Barhl2 morphants (*MObarhl2*) are shown at st. 27, st. 32 and st. 37 as indicated. Both the control (CT) and the injected (INJ) sides of a representative neural tube are shown, anterior left, dorsal up, allowing direct comparison of expression territories. *n*: number of embryos analyzed. The scale bar stands for 0.4 mm. In Barhl2-depleted embryos (A) the p3–p2 limit, marked by the caudal limit of the dorsal prethalamic marker *fezf2* ($n=24$), or (B) *arx2* ($n=24$) is established properly. The p2-like cells in *MObarhl2*-injected embryos are present and, at least in part, specified as shown by (C) the expression of the p2 basal plate marker *nkx2.1* ($n=16$), (D) that of *otx2* ($n=24$) and (E) *tcf4* ($n=20$). However, the p2 alar plate is misspecified: (F) the domain in which *pax6* is expressed spreads ventrally inside the mid-diencephalic furrow ($n=20$); In the rostral p2 (G) *irx3* expression remains unchanged compared to the CT side ($n=24$); Conversely (G) *irx3* expression is expanded in the caudal p2 of *barhl2*-depleted embryos ($n=24$), and expression levels of both caudal p2 markers (H) *irx1* ($n=24$) and (I) *irx2* ($n=36$) were down-regulated upon depletion of Barhl2 activity. (J) At st. 37 the progression of *shh* inside the p2 alar plate is inhibited ($n=16$).

the p2 alar plate, however, was abnormal in Barhl2 morphants: *pax6* was ectopically expressed in the mid-diencephalic furrow (Fig. 2F).

We focused our analysis on development of the p2 alar plate (Fig. 2G–J). In rostral part of p2 of Barhl2-depleted embryos, *irx3* was normally expressed (Fig. 2G); in the caudal p2 of these

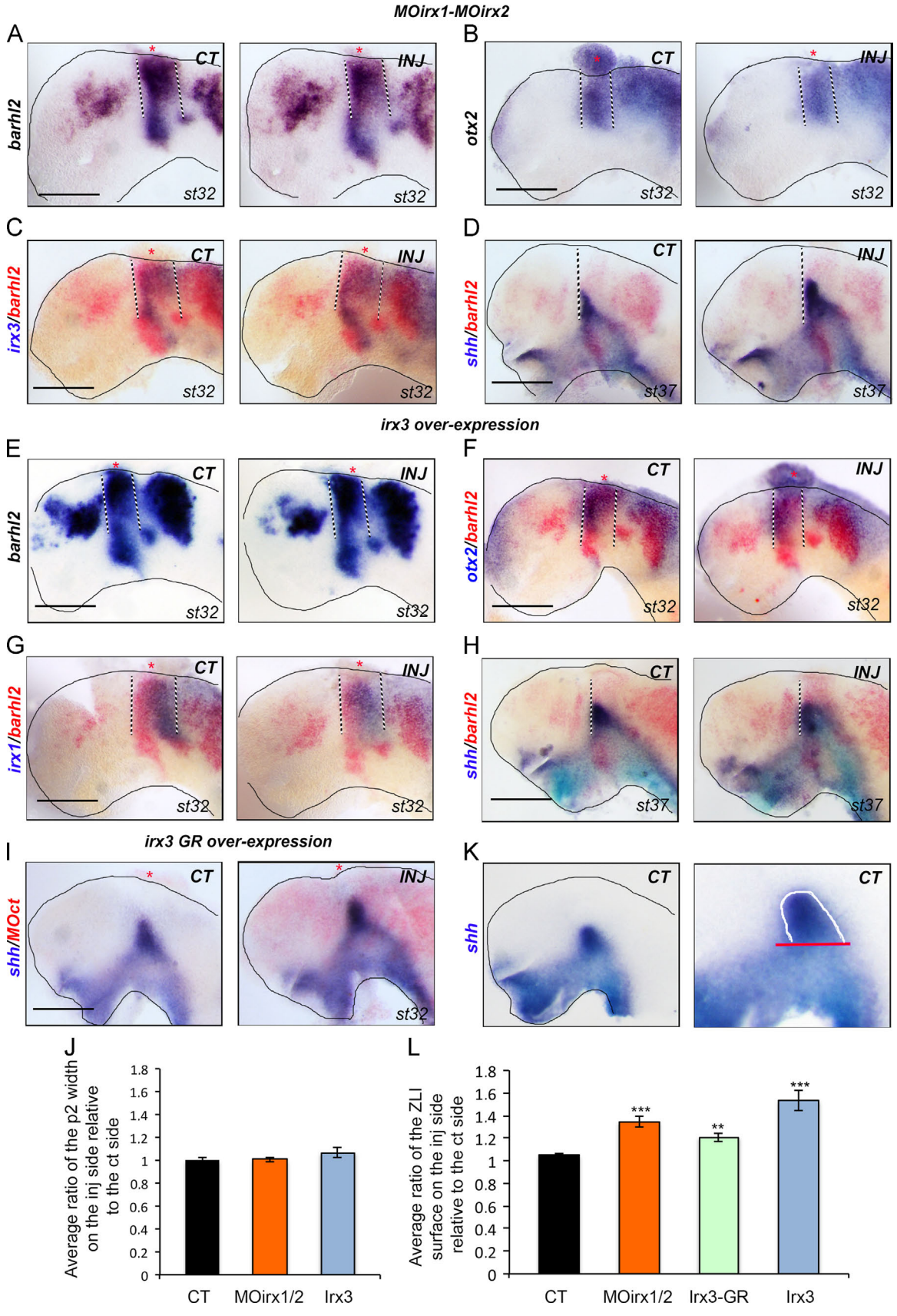

embryos, however, the *irx3* expression domain was enlarged (Fig. 2G), and the expression domains of *irx1* and *irx2* were decreased (Fig. 2H, I). We examined the impact of Barhl2 depletion on ZLI development and observed that the encroachment of *shh* delineating the forming ZLI did not appear in the p2 alar plate of Barhl2-depleted embryos (Fig. 2J).

We conclude that depletion of Barhl2 has no impact on either the establishment of the p2/p3 prosomeric limit or the basal p2 territory. However, Barhl2 depletion impairs the establishment of the p2 alar plate territories—the ZLI and caudal p2, without affecting *otx2* expression.

Depletion of Irx1/2 activity or overexpression of Irx3 promotes ZLI specification within the alar p2 territory

Before emergence of the ZLI, the rostral and caudal p2 domains differ in *irx* gene expression: the rostral p2 expresses *irx3* but not *irx1* or */2,* whereas the caudal p2 expresses all three *iroquois* genes. We investigated the respective contributions of *irx1/2* and *irx3* in ZLI development.

By using a mix of previously characterized MOs for both *irx1* (*MOirx1*) and *irx2* (*MOirx2*) (*MOirx1/2*) (Rodriguez-Seguel et al., 2009), we depleted Irx1/2 in the caudal forebrain and analyzed the formation of the p2 territory. We observed that *barhl2*, *otx2* and *irx3* expressions were only mildly impaired in Irx1/2-depleted embryos (Fig. 3A–C). Specifically the width of the p2 domain was not significantly changed in MOIrx1/2 injected embryos (Fig. 3A, J). Analysis of *shh* expression revealed a broadening of the ZLI territory (Fig. 3D, L). Double ISH analysis using *barhl2*, which marks p2, and *shh*, which marks the ZLI, revealed that in Irx1/2 double morphants the ZLI and *barhl2* rostral expression boundaries coincided precisely. Therefore, in *MOirx1/2*-injected embryos, the ZLI posterior boundary was caudally shifted.

We further investigated whether an increase in Irx3 activity in a territory co-expressing *barhl2* and *otx2* affects ZLI formation. We overexpressed Irx3 in *Xenopus* embryos and followed the formation of the p2 territory, the caudal p2, marked with *irx1/2,* and the ZLI. *barhl2* and *otx2* expressions were mildly impaired in these embryos and the width of the p2 domain was not changed (Fig. 3E–J). However, *irx1/2* expression was diminished (Figs. 3G and S2), and the surface of the ZLI territory was expanded. In most embryos the enlargement of the *shh* expression domain was associated to a decrease in the intensity of *shh* staining (Fig. 3H). We performed similar overexpression experiments using a hormone-inducible form of Irx3 (Irx3-GR) which activity was induced at stage 20 (Fig. 3I). We observed a slight broadening in the ZLI territory. Double ISH analysis, using *barhl2* and *shh*, demonstrated that the ZLI anterior border formed properly in these embryos (Fig. 3H). We quantified the expansion of the ZLI surface in MOirx1/2 injected, Irx3 and Irx3-GR overexpressing embryos and measured a significant increase of the ZLI area in all cases (Fig. 3K, L).

We conclude that within the p2 territory the loss of *irx1/2* or an increase in *irx3* expression promotes ZLI specification—i.e. in each case the number of cells that respond to the inductive influence of Shh by expressing *shh* is increased.

In explants the co-expression of barhl2, otx2 and irx3 enables neuroepithelial cells to express shh in response to a secreted form of Shh

In the developing neural tube the ZLI is the only part of the alar plate that expresses *shh.* Analysis of ZLI development in chick forebrain explants demonstrated that cells destined to become the ZLI initially occupy the alar plate and acquire their identity in response to Shh secreted from basal plate cells. Specifically Shh initiates in the ventral-most region of the alar plate the program of ZLI differentiation. Continuous Shh expression sustains the orthogonal progression of *shh* expression into the alar plate of p2 (Garcia-Lopez et al., 2004; Larsen et al., 2001; Zeltser et al., 2001). Here we investigated whether expression of *barhl2*, *otx2* and *irx3* i.e. pre-ZLI genes, in a neuroepithelial tissue acted on a cell's competence to express *shh* in response to a secreted form of Shh.

Animal cap explants (Anteriorized Animal Caps, AACs) prepared from *Xenopus* embryos injected with the BMP inhibitor *noggin* have previously been demonstrated to acquire an anterior neuroepithelial identity (Viczian and Zuber, 2010). AACs were prepared from embryos injected either with RNA encoding for *barhl2* and/or *otx2* and/or *irx3*, or with RNA encoding a secreted form of rat Shh (N-Shh). Using sandwich explants we mimicked inductive tissue interactions between the Shh-secreting basal plate and various neuroepithelial territories (Fig. 4A). We investigated the competence of neuroepithelial cells to express *shh* – *shh* from *Xenopus laevis* (*Xshh*), which does not cross-hybridizes with rat Shh – in response to a secreted form of Shh.

We first established that induction of *shh* does not occur in explants of either anterior, or p2-like, neuroepithelial identity cultured in the presence of N-Shh. Explants expressing *noggin* (anterior), or *noggin* together with *barhl2* and *otx2* (p2-like), genes were sandwiched with explants expressing N-Shh (Fig. 4B). We observed that AAC and p2-like explants exposed to N-Shh, did not express endogenous *Xshh* (Fig. 4Ba, b). Second we tested whether explants expressing *barhl2*, *otx2* and *irx3* – pre-ZLI – express *shh* in response to a secreted form of Shh. First, explants expressing

Fig. 3. Within alar p2, depletion of Irx1 and Irx2 activities, or an increase in Irx3 activity, promotes ZLI specification. Double ISH or ISH on embryos (A–D) either depleted for both Irx1 and Irx2 activities or (E–H) overexpressing *irx3*, or (I) overexpressing *irx3-GR* using *barhl2* (A, E), *otx2* (B, F), *irx3* (C), *irx1* (G), *shh* (D, H, I) probes as indicated. The scale bar stands for 0.5 mm. RNA encoding for *irx3,* or *irx3-GR* were co-injected with a MO control used as tracer, coupled to fluorescein detected by immunohistochemistry (*red*). **(**A–D**)** Co-depletion of Irx1/2 shifts the ZLI caudal border. In st. 32 embryos depleted for *irx1*/2 (A) *barhl2* ($n=24$) expression is not significantly affected, and (B) *otx2* ($n=20$) expression is slightly decreased. We observed (C) a weak increase of *irx3* in the thalamic domain ($n=36$). (D) The ZLI territory, characterized by *shh* expression, is enlarged ($n=36$); DISH using *barhl2* together with *shh* probes shows that the *barhl2* anterior border and the ZLI anterior border coincided, indicating that the ZLI posterior boundary is caudally shifted. **(**E–I**)** *irx3* or *irx3-GR* overexpression promotes ZLI specification. At st. 32 in *irx3* overexpressing embryos (E) *barhl2* ($n=40$) expression is modified compared with the CT sides whereas (F) *otx2* ($n=40$) and (G) *irx1* ($n=40$) expression are weakly decreased in the caudal p2 domain. (H) In *irx3* overexpressing embryos the surface of the ZLI territory marked by *shh* is enlarged ($n=22$). DISH using *barhl2* together with *shh* as probes demonstrates that the ZLI anterior border is not affected. Note that in embryos overexpressing Irx3 the expansion of the ZLI territory is associated to a decrease in *shh* staining intensity. (I) In embryos overexpressing a hormone-inducible form of *irx3* (irx3-GR) and exposed to dexamethasone at st. 20, the surface of the ZLI territory marked by *shh* is enlarged ($n=10$). (J) The average width of p2 is not modified in embryos depleted of Irx1/2 or overexpressing Irx3. Using *barhl2* as a p2 marker, the width of p2 was measured (Image J) on both the non-injected and the injected sides of embryos injected with GFP (CT, $n=11$), depleted for Irx1/2 (MOirx1/2, $n=12$) or overexpressing Irx3 (Irx3, $n=14$). The ratio of the p2 width of the injected side relative to the control side is shown. The error bars indicate the standard deviation. **(**K and L**)** The ZLI surface is significantly increased in Irx3 overexpressing embryos. (K) We delimited the alar/basal plate boundary of the diencephalon by drawing a line at the base of the ZLI area. We measure the ZLI area as the alar p2 area expressing *Xshh*. (L) Using Image J the surface of the ZLI territory was measured on both the non-injected and the injected sides of embryos injected with GFP (CT, $n=9$), overexpressing Irx3 (Irx3, $n=9$), or overexpressing a hormone-inducible form of Irx3 (Irx3-GR, $n=9$). The average ratio of the ZLI surface of the injected size relative to the control size is shown. The error bars indicate the standard deviation. We observed a significant increase of the ZLI surface in both Irx3 overexpressing embryos ($R=1.5\pm0.19$, *t*-test $p\leq0.004$) and Irx3-GR overexpressing embryos ($R=1.2\pm0.17$, *t*-test $p\leq0.03$).

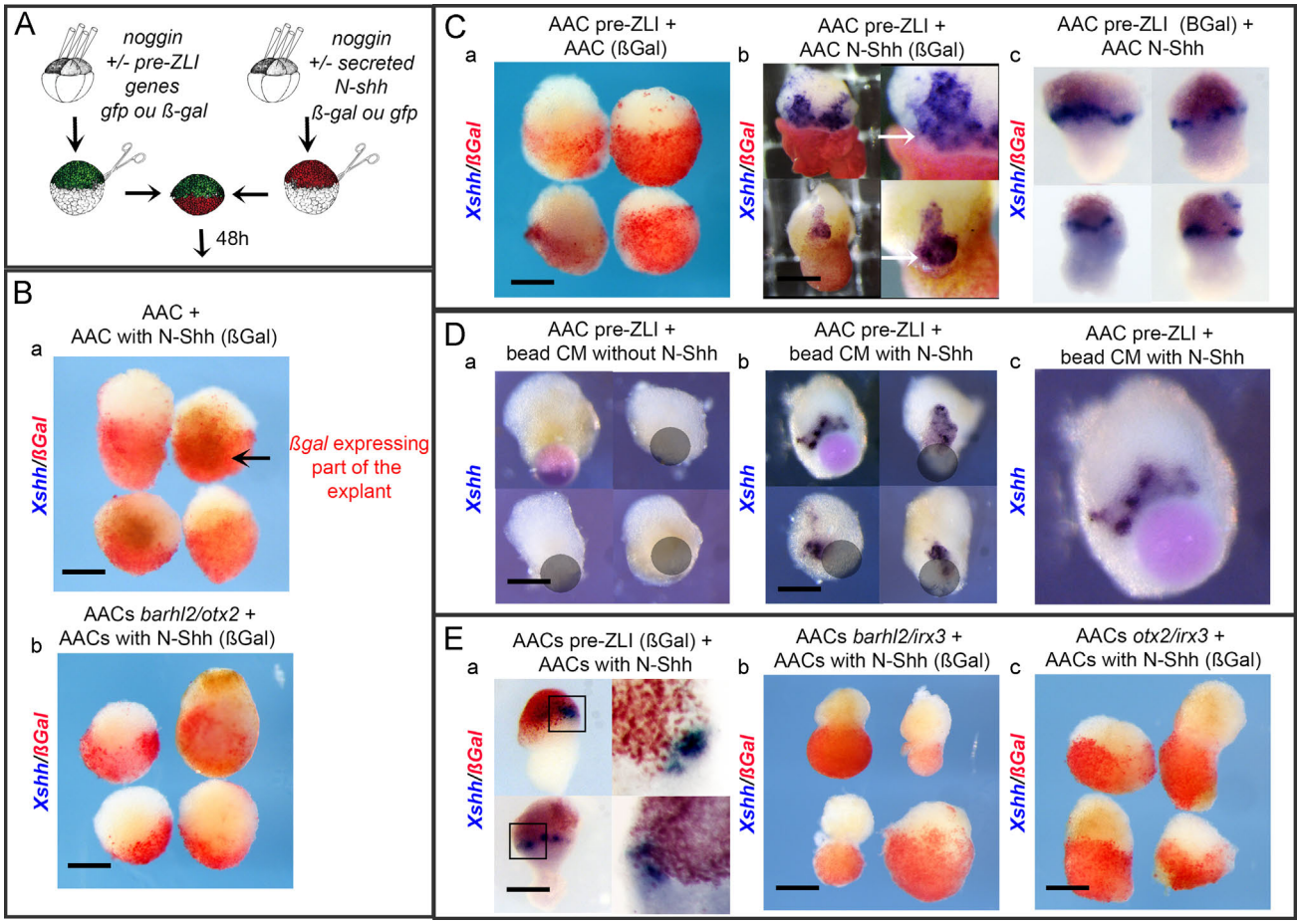

Fig. 4. In animal cap explants *barhl2, otx2* and *irx3* co-expression enables induction of *shh* expression by Shh. (A) Experimental design: AAC were prepared from embryos injected with RNA as indicated. AACs were sandwiched to yield ßGal/GFP conjugates and cultured for 48 h. In experiments shown in (D) the N-Shh-expressing part of the explant was replaced by beads. AACs were analyzed by ISH for expression of *Xenopus* (X) *shh*. The % of explants showing the phenotype is indicated. The scale bar stands for 0.5 mm. Representative sandwiched explants are shown. (B) Explants of anterior, or p2-like, neuroepithelial identity cultured in the presence of N-Shh are not competent to express *shh*. AACs expressing *noggin* (a) or *barhl2* and *otx2* (b) were sandwiched with AACs expressing N-Shh. Neither AACs (100%, $n=72$), nor p2-like explants (*barhl2*+*otx2*) (100%, $n=24$) expressed endogenous *Xshh* when exposed to N-Shh. (C, D) In the presence of N-Shh pre-ZLI's cells are competent to express *Xshh*. Pre-ZLI (*barhl2, otx2, irx3*) explants expressing or not ßGal (red) as indicated were sandwiched with: (C) (a) AACs (100%, $n=72$), or (b) AACs expressing N-Shh (b) (55%, $n=96$), (c) (72%, $n=25$). Enlarged image are shown in (b). Clusters of cells expressing *Xshh* appear along the border between the (*barhl2*, *otx2*, *irx3*)- and the Shh-expressing parts of the explants (white arrow). (D) beads (a) without N-Shh (88%, $n=25$) or (b) with N-Shh (76%, $n=25$). (c) Enlarged image of (b): clusters of cells expressing *Xshh* developed in close contact with the N-Shh-impregnated beads. The gray circle indicates the bead's location. (E) Induction of *Xshh* occurs within *barhl2, otx2, irx3* expressing cells and when any of the transcription factors *barhl2* or *otx2* or *irx3* is absent, *Xshh* expression is not induced in explants. (a) Pre-ZLI (*barhl2*, *otx2*, *irx3*) explants expressing ßGal (red) were sandwiched with AACs expressing N-Shh (72%, $n=25$). Representative explants and vibratome sections (30 μm) are shown. The *Xshh* expressing-cells exhibit ßGal activity. Representative sandwiched AACs are shown for: (b) AACs (*barhl2*+*irx3*) with AACs N-Shh (100%, $n=24$), (c) AACs (*otx2*+*irx3*) with AACs N-Shh (92%, $n=24$). The scale bar stands for 0.5 mm.

barhl2, *otx2* and *irx3* were sandwiched with explants expressing N-Shh, or not (Fig. 4C). Second, the same explants were left in contact with beads impregnated with a conditioned medium (CM) containing N-Shh, or the same CM preincubated with a Shh neutralizing antibody (Fig. 4D). After a period of 48 h that is the length of time necessary for sibling's embryos to develop a ZLI territory, we investigated whether these explants expressed endogenous *shh*. We observed the appearance of clusters of *Xshh*-expressing cells on explants left in contact with a source of N-Shh (Fig. 4Cb, c; Db, and c). The cluster of *Xshh*-expressing cells developed at the border with the explant's part expressing N-Shh (Fig. 4Cb, c). Importantly when the tracer (ßgal) was co-injected with *barhl2, otx2, irx3*, the *Xshh* expressing-cells exhibited ßGal activity (Fig. 4Ea). When any of the transcription factor genes *barhl2, otx2, irx3*, was not expressed, we did not observe induction of *Xshh* expression (Fig. 4Bb, Eb, and c).

We conclude that in explants the co-activity of Barhl2, Otx2 and Irx3 plays a key role in enabling the ability to respond to the inductive influence of N-Shh by expressing *shh*. Specifically the activity of each of these transcription factors is necessary, at least in initiating the ZLI differentiation program in the starting neural cell population.

Neuroepithelial cells coexpressing barhl2, otx2 and irx3 show Shh-dependent segregation

Formation of the ZLI territory correlates with the acquisition of cell lineage restriction properties at both its anterior and posterior borders. We investigated whether expression of *barhl2*, *otx2*, *irx3* genes acted on a neuroepithelial cell's ability to segregate from its neighboring territories—either from anterior neuroepithelial cells marked by the expression of *otx2* (Blitz and Cho, 1995) or from thalamus cells marked by the expression of *barhl2*, *otx2*, *irx1* and *irx2*. In both cases, we evaluated the impact of Shh on cells expressing *barhl2*, *otx2* and *irx3* (i.e. rostral p2-like cells) segregation behavior.

We generated AACs as above or prepared them from embryos injected either with *otx2*, or with *barhl2*, *otx2* and *irx3* marked with ßGal (red) or with thalamus genes (Fig. 5). When necessary,

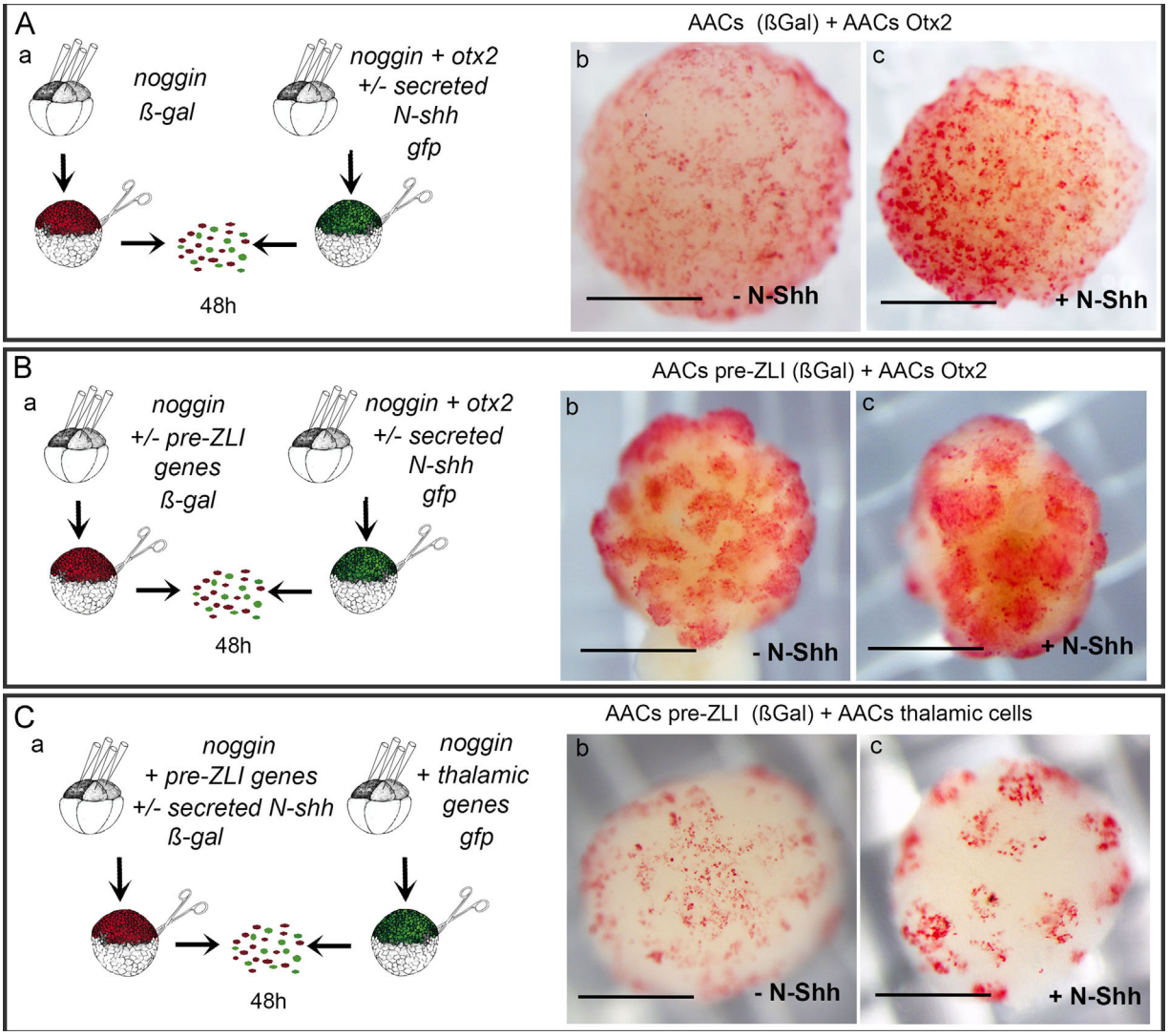

Fig. 5. In reaggregated explants cells expressing pre-ZLI genes exhibit Shh-dependent segregation behaviors: (a) Experimental design: AAC were prepared from embryos injected as indicated. At st. 8/9 *ßgal* and *gfp* cells are dissociated and reaggregated to generate explants made of Gfp/ßGal (red) mixed cell types. The explants are cultured for 48 h. (b, c) Representative explants composed of mixed cells expressing the different neuroepithelial genes as indicated are shown (b) without N-Shh (c) with N-Shh (100%, $n \geq 10$ for each condition). The % of explants showing the phenotype is indicated. The scale bar stands for 0.5 mm. (A) AAC cells do not segregate from Otx2-expressing cells. AACs cells expressing *otx2* spread randomly when mixed with AACs cells (red) (b) in the absence (100%, $n=12$) and (c) in the presence of N-Shh (100%, $n=10$). (B) Pre-ZLI-like cells segregate from Otx2-expressing cells. Pre-ZLI cells (red) regrouped and separated from anteriorized neuroepithelial cells in the absence (b) and presence (c) of N-Shh (100%, $n=10$ for each condition). (F) In the presence of N-Shh pre-ZLI-like cells segregate from thalamus-like cells (b, c) pre-ZLI cells (red) regrouped, and separated from thalamus-like cells in the presence (c) but not in the absence (b) of N-Shh (100%, $n=10$ for each condition).

RNA encoding a secreted form of Shh was injected as indicated (Fig. 5). We made use of the ability of animal cap explants to be dissociated and immediately re-aggregated to generate explants composed of mixed neuroepithelial cells expressing the different neuroepithelial signatures. We observed that AAC cells mixed with *otx2*-expressing cells, intermingled freely in the absence or in the presence of N-Shh (Fig. 5A). In contrast, rostral p2-like cells separated from *otx2*-expressing cells in the presence and in the absence of N-Shh (Fig. 5B). Finally, we observed that the rostral p2-like cells coalesced and separated from thalamic cells in the presence, but not in the absence, of N-Shh (Fig. 5C).

We conclude that expression of *barhl2, otx2, irx3* genes enables cells to segregate from cells of other anterior neural lineages, except those expressing thalamus genes i.e. *barhl2*, *otx2*, *irx1* and *irx2*; moreover, secreted Shh enables the ability of rostral p2-like cells to sort-out from thalamus-like cells.

In explant sandwiches rostral p2-like cells, and thalamus-like cells recapitulate the main features of their in vivo developmental program

From st. 30 to st. 37, the expression of *barhl2* and *otx2* in the p2 alar plate remained stable. In contrast, the expression pattern of *irx3* changed: at st. 30, the *irx3* expression domain encompassed the entire alar p2, but it progressively narrowed to the rostral p2, and by st. 37 *irx3* was expressed in the ZLI and in the epithalamus (Figs. 1M, N and S3). Thus, the restricted expression of *irx3* coincided in time with the segregation of the ZLI and thalamic territories. We therefore investigated the behavior of *barhl2, otx2, irx3* expressing cells when in contact with a thalamus-like tissue.

Using explant sandwiches as described earlier, we simulated interactions between the pre-ZLI and the thalamus in the presence or absence of N-Shh (Fig. 6A and B). We tested whether the explants expressed *Xshh*, whether the pre-ZLI-like or the thalamic-like cells

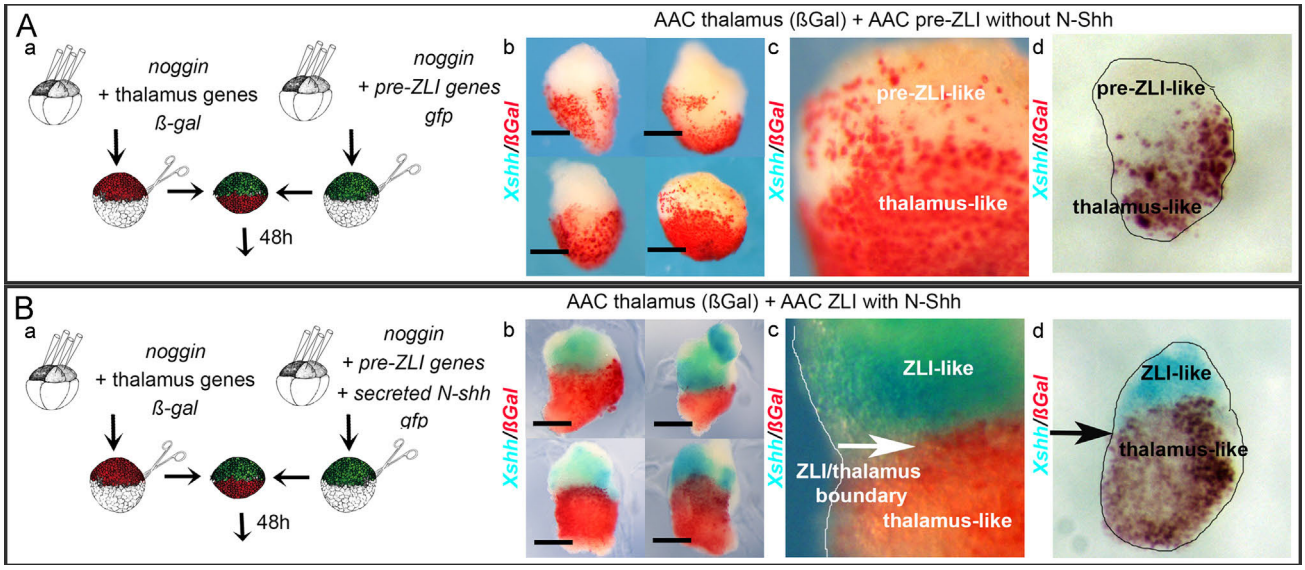

Fig. 6. In pre-ZLI-like/thalamus-like explant sandwiches, cells recapitulate the main features of their *in vivo* developmental program. (A, B) In sandwiched explants pre-ZLI-like cells segregate and form a boundary with thalamus-like cells in the presence of N-Shh. (a) Experimental design: cRNA were injected as indicated. (b, c) Representative explants of thalamus-like AACs (red) sandwiched with pre-ZLI-like AACs without (A) or with (B) N-Shh. (A) In the absence of N-Shh pre-ZLI-like cells did not express *Xshh* and intermingled with thalamic-like cells. (c) Enlarged views and (d) section, of a representative explant. In contrast (B) in the presence of N-Shh pre-ZLI-like cells expressed *Xshh* and formed a boundary with thalamus-like cells (85%, $n=15$). (c) Enlarged views and (d) section, of a representative explant.

expressed *Xshh*, and whether the pre-ZLI-like and thalamic-like part of the explant sandwich formed a boundary.

In the absence of Shh, neither rostral p2-like nor thalamic-like cells expressed *Xshh,* and both type of cells intermingled (Fig. 6Ab–d). In contrast, in the presence of N-Shh, patches of *Xshh*-expressing cells appeared in the explants, but only in the pre-ZLI-like half of the sandwich: the *Xshh* expressing-cells did not exhibit ßGal activity, the thalamic cells tracer. In agreement with our previous observations, in the presence of N-Shh, we observed a clear boundary between the thalamus-like and rostral p2-like tissues (Fig. 6Bb–d).

We conclude that the *barhl2*, *otx2*, *irx3* expressing cells i.e. rostral p2-like cells, and *barhl2*, *otx2*, *irx1* and *irx2* i.e. thalamus-like cells recapitulate the main features of their *in vivo* developmental program in our explant sandwiches.

In a developing neuroepihelium, when continuously exposed to N-Shh, cells expressing barhl2, otx2 and irx3 form ectopic ZLI

Our above findings established that, in explants, cells expressing *barhl2*, *otx2*, *irx3* can be induced by Shh to acquire two key developmental features of the ZLI: the competence to express *shh* and the ability to segregate from their neighboring territories.

We further investigated the behavior of cells ectopically expressing *barhl2*, *otx2*, *irx3* and continuously exposed to Shh *in vivo*. We generated mixed explants composed of N-Shh-expressing cells mixed with otx2- (Otx2–N-Shh), or *barhl2*, *otx2*, *irx3*- (BOI3–N-Shh) expressing cells (Fig. 7). Pieces of explants were grafted into the neural plate of st. 14 *Xenopus* embryos. The grafted cells were marked with ßGal (red). At st. 35 we analyzed (i) whether grafted cells expressed *Xshh*, (ii) whether the cells ectopically expressing *Xshh* segregated from their neighbors, (iii) whether these “ectopic ZLI” structures developed with or without a contact with an endogenous source of N-Shh – the floor or basal plates, the ZLI. Whereas in (Otx2–N-Shh) grafted embryos we did observed formation of ectopic ZLI (Fig. 7B and C), most of (BOI3–N-Shh) grafted embryos exhibited one, and up to five, ectopic ZLIs i.e. a cluster of cells expressing *Xshh* (Fig. 7B and C). 40% of these “ectopic ZLI” developed without any contact with an endogenous source of N-Shh (Fig. 7C).

Finally we investigated whether the ectopic expression of *barhl2*, *otx2*, *irx3* drove cells from the anterior neuroepithelial plate to acquire a ZLI identity. *Xenopus* embryos were injected at the 16-cell stage in one dorsal blastomere with RNA encoding *barhl2*, *otx2*, *irx3* together with RNA encoding ßGal used as a tracer. When in contact with the floor plate or the basal plate (i.e., a source of secreted Shh), cells ectopically expressing rostral p2-like signature formed cell clusters. In some of these clusters, we detected *Xshh* expression, mimicking ZLI formation (Fig. 7Db, c).

We conclude that when continuously exposed to Shh signal, neuroepithelial cells co-expressing *barhl2*, *otx2*, *irx3* form ectopic ZLI.

Barhl2 role in p2 patterning partly depends on Barhl2's ability to control the levels and stability of ß-Catenin

We previously demonstrated that *barhl2* limits p2 neuroepithelial cell proliferation and plays a part in the maintenance of diencephalic neuroepithelial architecture by tightly controlling the levels and stability of ß-Catenin (Juraver-Geslin et al., 2011). We investigated whether a reduction in ß-Catenin can rescue the p2 patterning defects in Barhl2-depleted embryos. We followed *pax6*, *irx1*/2 and *shh* expression in Barhl2-depleted and Barhl2/ßCat double morphants embryos. Co-injection of MOs against *barhl2* and *ßcat* resulted in a normalization of the patterning defects in p2 alar plate markers (Fig. 8A–C): specifically, we observed a decrease in ectopic *pax6* expression in the mid-diencephalic furrow (Fig. 8A) and the decrease in *irx1*/2 expression observed in the neural tube of Barhl2-depleted embryos was partly rescued in Barhl2/ßCat-doubly depleted embryos (Fig. 8B and C).

We further investigated whether depletion of ß-catenin in Barhl2 morphants rescued ZLI development. We compared *shh* expression in Barhl2-depleted and Barhl2/ßCat double morphants embryos. We did not observe any significant rescue of ZLI formation in Barhl2/ßCat double morphants embryos (Fig. 8D). Note that in Barhl2 morphants Barhl2 protein was absent.

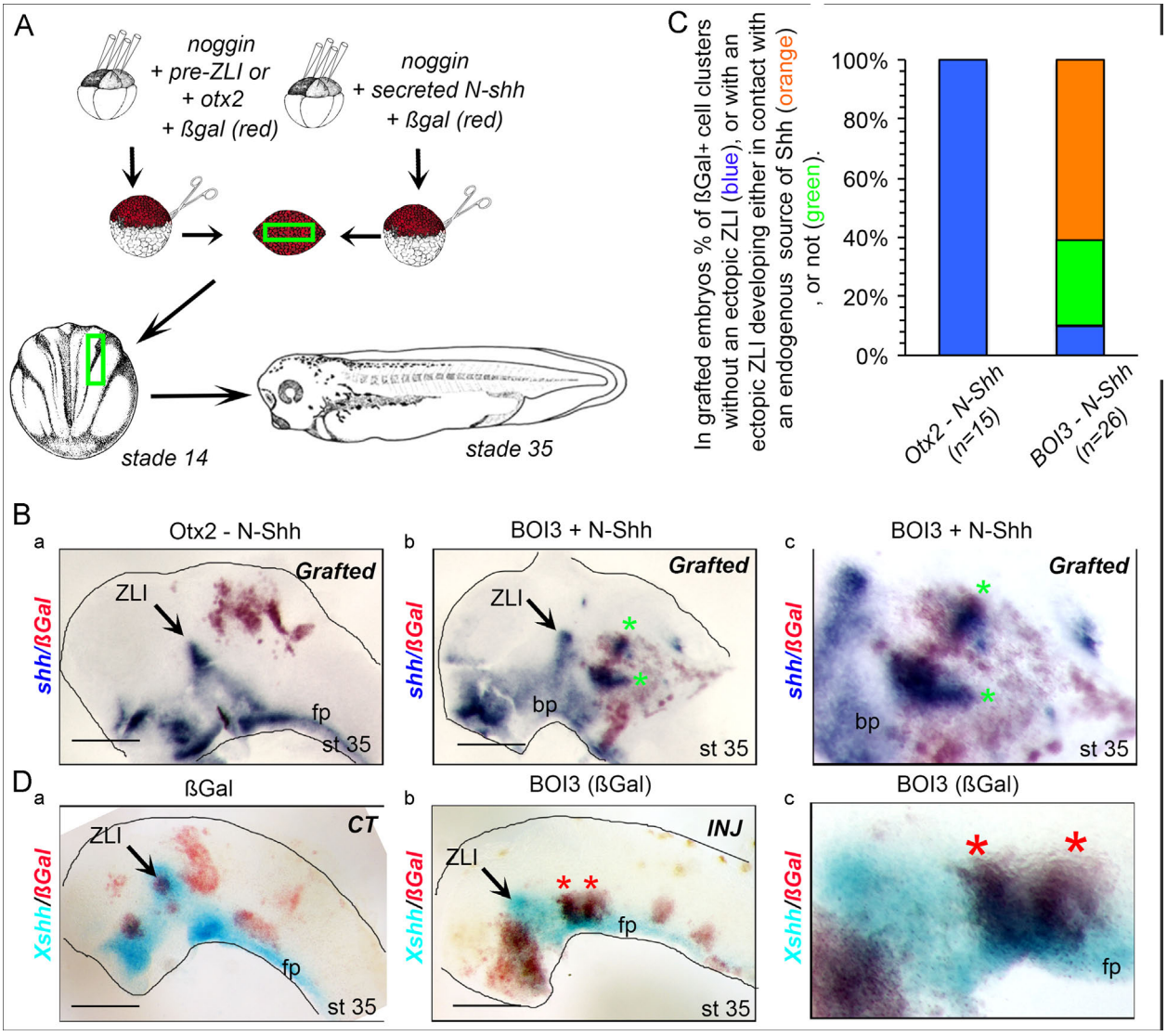

Fig. 7. When ectopically expressed in the developing neuroepithelium and continuously exposed to Shh, pre-ZLI-like cells recapitulate the characteristic features of their developmental program. (A) Experimental design: AAC were prepared from embryos injected with RNA as indicated. At st. 8/9 cells were dissociated and reaggregated to generate explants made of mixed cell types. Pieces of explants were grafted into sibling's neural plate at st. 14. Embryos were let to develop until st. 35. (B, C) Grafted cells expressing *barhl2*, *otx2*, *irx3* develop ectopic ZLI when continuously exposed to Shh. (B) ISH using *Xshh* as probe on st. 35 embryos grafted with AACs (*otx2*+N-Shh) (a), or AACs (*barhl2*, *otx2*, *irx3*+N-Shh) (b) mixed explants. The grafted sides of st. 35 representative neural tubes are shown, side view, dorsal up, anterior left. ZLI: *zona limitans intrathalamica*; fp: floor plate. (c) Enlarged view of grafted cells from (b). (C) Analysis of grafting experiments. In embryos grafted with (*otx2*+N-Shh) mixed explants no ectopic ZLI develop in ßGal-expressing cell clusters (shown in blue) (100%, $n=18$). In contrast in embryos grafted with (*barhl2*, *otx2*, *irx3*+N-Shh) mixed explants most embryos developed ectopic ZLI (89%, $n=26$). From 35 identified ectopic ZLI, 25 developed in contact with an endogenous source of Shh – floor or basal plates, the ZLI – (shown in orange) and 10 developed autonomously (shown in green). (D) Injected pre-ZLI cells develop ectopic ZLI when continuously exposed to Shh. ISH using *Xshh* as probe on st. 36 embryos injected into the same dorsal blastomere of 16-cell stage embryos with (a) *ßgal* alone, or together with *barhl2*, *otx2*, *irx3* genes (b, c). The injected sides of st. 36 neural tubes are shown, side view, dorsal up, anterior left. When in contact with a source of secreted Shh, pre-ZLI-like cells (red) formed cellular clusters inside which *Xshh* expression is detected (stars). (c) Enlarged view of an "ectopic ZLI".

We conclude that whereas depletion of ß-Catenin rescues some p2 patterning defects in Barhl2-depleted embryos, it does not rescue Barhl2 ability to contribute to the ZLI specification process.

Discussion

Barhl2 acts downstream of otx2 and together with irx3 in ZLI formation

In this study, we performed a detailed analysis of alar prosomere p2 development in *Xenopus laevis* embryos. We uncover a new role for Barhl2 in diencephalic patterning. We demonstrate that Barhl2 activity is required for fate determination of both the ZLI and the thalamus. Within the p2 territory that expresses *barhl2* and *otx2*, overexpression of Irx3 or depletion of Irx1/2, promotes the acquisition of a ZLI fate at the expense of a thalamic fate. Therefore, the ratio of Irx3 to Irx1/2 in p2 cells has a decisive role in specifying the ZLI and its size. Zebrafish embryos that are deficient in both Otx1l and Otx2 proteins resemble Barhl2-depleted *Xenopus* embryos: although most forebrain markers are unaltered, the embryos exhibit defects in *shh* expression in the ZLI, in the formation of the mid-diencephalic furrow, and in *barhl2* expression starting at the 12-somite stage (Scholpp et al., 2007). Therefore, Otx1l/2 proteins maintain expression of *barhl2* in the future ZLI territory, and the loss of *barhl2* contributes to the ZLI defects observed in Otx-deficient zebrafish.

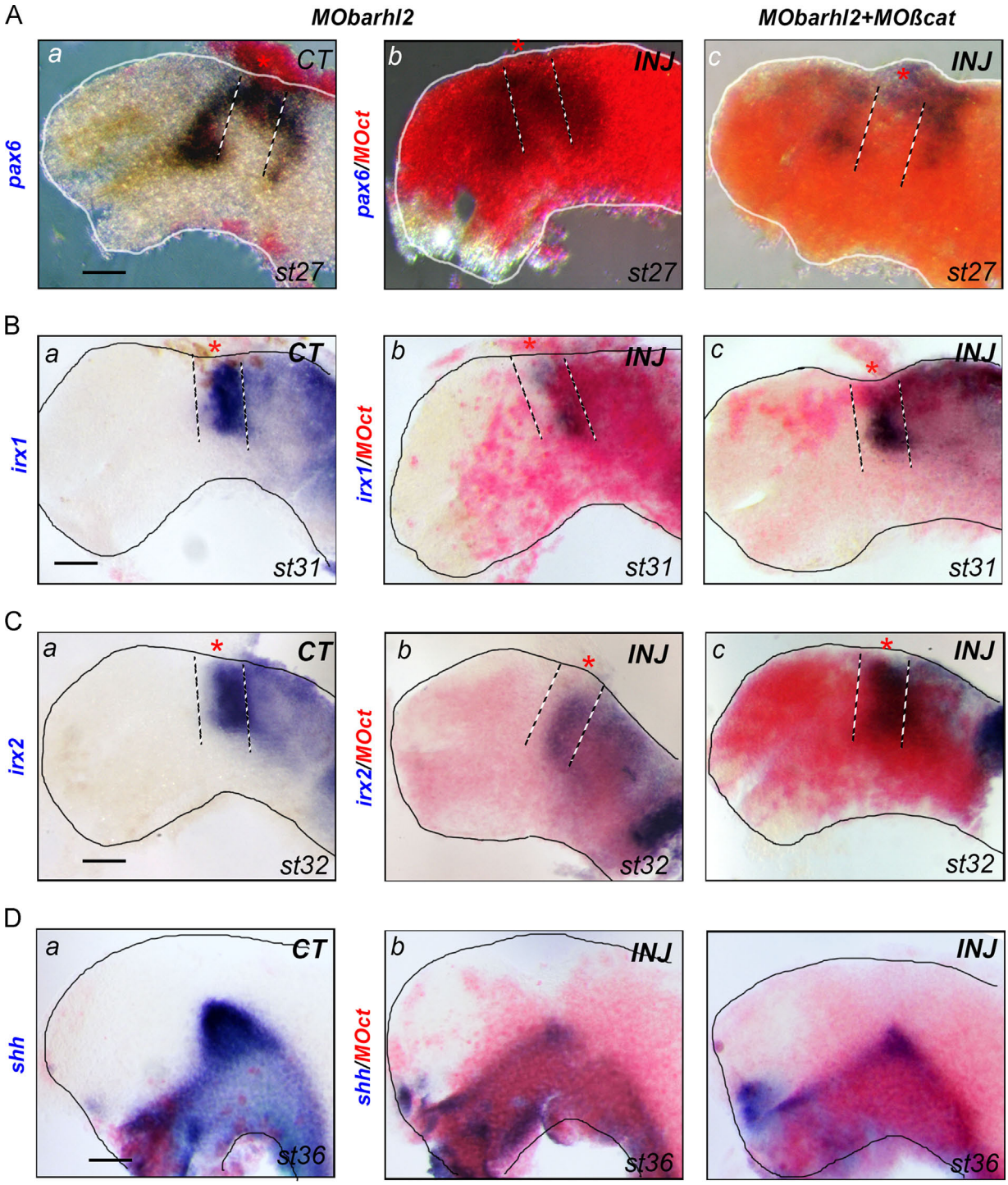

Fig. 8. Some patterning defects observed in Barhl2 depleted embryos are rescued by decreasing ß-catenin levels, but not ZLI development. (A–D) ISH on embryos depleted for *barhl2* (a, b) or both *barhl2* and *ßcatenin* (c) using *pax6* (A), *irx1* (B), *irx2* (C), and *shh* (D) as probes. The CT (*MObarhl2*) and rescued (*MObarhl2/MOßcat*) embryos were generated during the same set of experiments, and were coinjected with a MO control used as tracer, coupled to fluorescein detected by immunochemistry (red). For *MObarhl2/MOßcat* injected embryos, only the injected side is shown. The scale bar stands for 0.2 mm. (E–I) Barhl2 depletion patterning defects are partly rescued by decreasing ß-catenin levels. Barhl2 depletion phenotypic defects, specifically (A) *pax6* ectopic expression in the mid-diencephalic furrow ($n=25$), (B, C) the decrease of *irx1* ($n=20$) and *irx2* ($n=22$) thalamic expression are partly rescued by depletion of *ßcat*. (D) The loss of ZLI development observed in Barhl2-depleted embryos is not rescued by decreasing ß-catenin levels. At st. 37 the progression of *shh* inside the p2 alar plate is inhibited in both Barhl2 depleted embryos (b, $n=36$) and Barhl2/ßCat double morphants embryos (c, $n=36$).

We demonstrate that when continuously exposed to secreted Shh, neuroepithelial cells co-expressing *barhl2*, *otx2* and *irx3*, both in explants and in grafted embryos, acquire two characteristics of the ZLI compartment: the competence to express *shh* and the ability to segregate from anterior neural plate cells. Therefore *barhl2* acts downstream of *otx2* and, together with *irx3*, enables the cells to acquire pre-ZLI properties. Note that in the present study we consider the pre-ZLI to be the alar p2 territory expressing *barhl2*, *otx2*, *irx3* before *shh* expression. This definition is different from that described in chick, which defines the pre-ZLI as a wedge-shaped prosencephalic

compartment characterized by the expression of *wnt8b* and a gap in the expression of Lunatic-Fringe (LFng), a glycosyltransferase that regulates Notch signaling (Zeltser et al., 2001).

Genetic programs for body patterning that are homologous to ancestral organizing centers are present in the deusterostome *S.Kowalevskii*. In this hemichordate, which appears to be closest to the central basic reference animal at the root of the chordate phylogenetic tree, the Barhl2 ortholog, BarH, is present at the right time and place relative to *hedgehog*, *otx* and *irx* orthologs to perform its role in patterning the body plan (Lowe et al., 2003; Pani et al., 2012). Therefore, at least parts of the genetic network controlling ZLI specification that we describe in amphibian are evolutionarily conserved.

Shh induces the cell segregation that helps partitioning p2

We provide evidence that in amphibians a dynamic process, concomitant in time with ZLI formation, leads to the separation of the p2 histogenic field into two caudal forebrain territories: the ZLI, which expresses *barhl2*, *otx2*, *irx3* and *shh*, and the thalamus, which expresses *barhl2*, *otx2* and *irx1/2*. Similar to the chick but in contrast to the zebrafish, we establish that induction of *shh* expression within the ZLI in amphibian embryos requires the continuous presence of Shh (Scholpp et al., 2007; Vieira and Martinez, 2006; Zeltser, 2005). Our results also argue that Shh plays an important part in establishing the ZLI/thalamus boundary. In both reaggregated and sandwiched explants, in the absence of Shh, pre-ZLI cells sort out from anterior neuroepithelial cells but not from cells expressing a thalamus gene signature. In contrast, in the presence of Shh, pre-ZLI and thalamus cells sort out in such explants. During early neurulation, *otx2*, *barhl2* and the *irx* genes are co-expressed in p2 and are the earliest specific markers of p2 (Offner et al., 2005; Rodriguez-Seguel et al., 2009). Whereas at the onset of ZLI formation *irx3* is expressed in the alar part of p2, at the end of ZLI development the *irx3* expression territory is shifted rostrally into the ZLI compartment and *irx1* and *irx2* expression domains are restricted to the thalamus territory. Further work is necessary to establish whether Shh induces the segregation of ZLI and thalamus cells *in vivo* and to assess whether Irx proteins regulate one another's expression. However, our results demonstrate that, in amphibians, Shh is strictly necessary for both induction of *shh* expression within the ZLI and formation of the ZLI caudal border. Overexpression of Irx3 generates an enlargement of the ZLI associated to a decrease in the intensity of *shh* staining. In the ZLI/thalamic explant sandwiches, the efficiency of the *shh* induction process—i.e., the average size of the *shh*-expressing areas—was increased compared with that observed in pre-ZLI explants exposed to N-Shh. It is therefore possible, however not deciphered, that the thalamus territory facilitates the induction of *shh* and contributes to the dorsal progression of *shh* expression within the ZLI.

In mouse and zebrafish, the ZLI anterior boundary is established at the p2/p3 border through cross-inhibitory interactions between Fezf2 and Irx3 (Hirata et al., 2006; Jeong et al., 2007; Rodriguez-Seguel et al., 2009; Scholpp et al., 2007). In amphibians, Barhl2-depleted embryos do not display any defect in the establishment of the p2/p3 limit, and the ZLI develops within p2 between st. 30 and st. 37. By analogy with the induction of the Midbrain–Hindbrain Boundary, which develops at the interface of expression of *otx2* and *gbx2*, it has been suggested, but not directly tested, that the interface between *fezf2* and *irx3* expression domains is the inductive cue at the origin of ZLI formation (reviewed in Epstein, 2012; Hagemann and Scholpp, 2012; Kiecker and Lumsden, 2005; Martinez-Ferre and Martinez, 2012; Scholpp and Lumsden, 2010). Our findings argue that, at least in amphibians, the p2/p3 border is established before ZLI development and may not be responsible for ZLI induction (Hirata et al., 2006; Jeong et al., 2007; Kobayashi et al., 2002).

Barhl2 activity that cell-autonomously limits canonical Wnt activity contributes to ZLI development

We previously demonstrated that *barhl2* acts as a brake on p2 neuroepithelial cell proliferation, and that it plays a part in the maintenance of diencephalic neuroepithelial architecture by tightly controlling the levels and stability of ß-Catenin (Juraver-Geslin et al., 2011). In Barhl2-depleted embryos, alterations in *pax6* and *irx1*/2 expression levels in the p2 alar plate are compensated for by a depletion of ß-catenin. Therefore, Barhl2's role in limiting ß-catenin levels plays a part in patterning the alar p2. Analysis of caudal forebrain proliferation kinetics in chick and mice reveal that ZLI cells divide slowly relative to cells in their flanking territories (Baek et al., 2006; Martinez and Puelles, 2000). Cells of neighboring compartments separate along boundaries, most probably based on differences in their adhesive properties (reviewed in Dahmann et al., 2011; Kiecker and Lumsden, 2005). Besides its documented role in controlling neuroepithelial cell proliferation, ß-Catenin acts on thalamic cell adhesiveness and segregation by mediating the interactions between the intracellular cytoskeleton and the Cadherins, a group of cell–cell adhesion proteins important in the formation of neural boundaries (Peukert et al., 2011; Puelles, 2007; Redies, 2000). Therefore, our data support a conserved function for Barhl2 in limiting the rate of cell proliferation and modulating cell adhesion in the ZLI territory.

In chick the dorsal forebrain territory expressing *wnt8b* has been suggested to delimitate the pre-ZLI territory (Zeltser et al., 2001), and a Wnt8b-induced Wnt signal is a prerequisite for the induction of *shh* expression and for ZLI emergence in the diencephalic primordium (Martinez-Ferre et al., 2013). In zebrafish, *wnt3* and *wnt3a* are co-expressed in the ZLI anlage, and their early depletion affects its induction (Mattes et al., 2012). In *Drosophila*, *barH* and *wingless* appear to regulate each other's expression: Wg activates BarH and BarH represses Wg (Sato et al., 1999). Further work is necessary to identify the inductive signals underlying the induction and/or stabilization of *barhl2, otx2* and *irx* expression in the neural plate caudal forebrain territory, and to decipher the complex interactions between Barhl2, Otx2, Irx, and the Wnt and Shh signaling pathways at play during ZLI elaboration. However a role for Wnt ligands in controlling the transcription and/or protein stability of *barhl2* and *irx3* could contribute to the role of Wnt signaling in ZLI development.

Conclusion

In conclusion our study uncover a new role for the conserved *barhl2* gene: *barhl2* acts downstream of *otx2* and in concert with *irx3* in the developmental program controlling ZLI formation. At least in amphibians, the ZLI develops within the prosomere p2 and, when continuously exposed to Shh, a neuroepithelial territory coexpressing *barhl2*, *otx2* and *irx3* transcription factors develops key ZLI developmental features.

Acknowledgments

We thank M. Wassef, J. Collignon, A.H. Monsoro-Burq, S. Schneider-Maunoury for their comments on the manuscript. R.J. Wechsler-Reya, D. Gradl, D. Dupasquier, R. Moon, S. Ekker, W.A. Harris, H. Sive, R. Vignali, Y. Sasai, N. Papalopulu, K. Koebernick, J.L. Christian, E.M. De Robertis, T. Pieler, E.J. Bellefroid, H.M. El-Hodiri, A.M. Zorn, L. Kodjabachian, P.A. Krieg, M. Perron, R.M. Harland, S. Rétaux, M. Umbhauer, M. Whitman, M. Jamrich, for generous gifts of probes and expression

vectors. The Xenbase data base (James-Zorn et al., 2013; Bowes et al., 2008). "The English Edition" and Martin Raff for their editing work on the manuscript. This work was supported by the Centre National de la Recherche Scientifique (CNRS UMR8197, INSERM U1024) and by grants from the Fondation Pierre Gilles de Gennes (FPGG0039), the "Association pour la Recherche sur le Cancer" (ARC 4972 and ARC 5115 to M.W.; FRC DOC20120605233 and LABEX Memolife to H.J.G.).

Appendix A. Supporting information

Supplementary data associated with this article can be found in the online version at http://dx.doi.org/10.1016/j.ydbio.2014.09.027.

References

Baek, J.H., Hatakeyama, J., Sakamoto, S., Ohtsuka, T., Kageyama, R., 2006. Persistent and high levels of Hes1 expression regulate boundary formation in the developing central nervous system. Development 133, 2467–2476.
Blitz, I.L., Cho, K.W., 1995. Anterior neurectoderm is progressively induced during gastrulation: the role of the Xenopus homeobox gene orthodenticle. Development 121, 993–1004.
Bowes, J.B., Snyder, K.A., Segerdell, E., Gibb, R., Jarabek, C.J., Pollet, N., Vize, P.D., 2008. Xenbase: a Xenopus biology and genomics resource. Nucleic Acids Research 36 (suppl 1), D761–D767.
Chatterjee, M., Li, J.Y., 2012. Patterning and compartment formation in the diencephalon. Front. Neurosci. 6, 66.
Coffman, C., Harris, W., Kintner, C., 1990. Xotch, the Xenopus homolog of Drosophila notch. Science 249, 1438–1441.
Dahmann, C., Oates, A.C., Brand, M., 2011. Boundary formation and maintenance in tissue development. Nat. Rev. Genet. 12, 43–55.
Epstein, D.J., 2012. Regulation of thalamic development by sonic hedgehog. Front. Neurosci. 6, 57.
Ericson, J., Morton, S., Kawakami, A., Roelink, H., Jessell, T.M., 1996. Two critical periods of Sonic Hedgehog signaling required for the specification of motor neuron identity. Cell 87, 661–673.
Figdor, M.C., Stern, C.D., 1993. Segmental organization of embryonic diencephalon. Nature 363, 630–634.
Garcia-Lopez, R., Vieira, C., Echevarria, D., Martinez, S., 2004. Fate map of the diencephalon and the zona limitans at the 10-somites stage in chick embryos. Dev. Biol. 268, 514–530.
Gomez-Skarmeta, J.L., Campuzano, S., Modolell, J., 2003. Half a century of neural prepatterning: the story of a few bristles and many genes. Nat. Rev. Neurosci. 4, 587–598.
Hagemann, A.I., Scholpp, S., 2012. The tale of the three brothers – Shh, Wnt, and Fgf during development of the thalamus. Front. Neurosci. 6, 76.
Harland, R.M., 1991. In situ hybridization: an improved whole-mount method for Xenopus embryos. Methods Cell Biol. 36, 685–695.
Hashimoto-Torii, K., Motoyama, J., Hui, C.C., Kuroiwa, A., Nakafuku, M., Shimamura, K., 2003. Differential activities of Sonic hedgehog mediated by Gli transcription factors define distinct neuronal subtypes in the dorsal thalamus. Mech. Dev. 120, 1097–1111.
Heasman, J., Kofron, M., Wylie, C., 2000. Beta-catenin signaling activity dissected in the early Xenopus embryo: a novel antisense approach. Dev. Biol. 222, 124–134.
Hirata, T., Nakazawa, M., Muraoka, O., Nakayama, R., Suda, Y., Hibi, M., 2006. Zinc-finger genes Fez and Fez-like function in the establishment of diencephalon subdivisions. Development 133, 3993–4004.
Hoch, R.V., Rubenstein, J.L., Pleasure, S., 2009. Genes and signaling events that establish regional patterning of the mammalian forebrain. Semin. Cell Dev. Biol. 20, 378–386.
James-Zorn, C., Ponferrada, V.G., Jarabek, C.J., Burns, K.A., Segerdell, E.J., Lee, J., Snyder, K., Bhattacharyya, B., Karpinka, J.B., Fortriede, J., Bowes, J.B., Zorn, A.M., Vize, P.D., 2013. Xenbase: expansion and updates of the Xenopus model organism database. Nucleic Acids Research 41 (D1), D865–D870.
Jeong, J.Y., Einhorn, Z., Mathur, P., Chen, L., Lee, S., Kawakami, K., Guo, S., 2007. Patterning the zebrafish diencephalon by the conserved zinc-finger protein Fezl. Development 134, 127–136.
Juraver-Geslin, H.A., Ausseil, J.J., Wassef, M., Durand, B.C., 2011. Barhl2 limits growth of the diencephalic primordium through Caspase3 inhibition of beta-catenin activation. Proc. Natl. Acad. Sci. USA 108, 2288–2293.
Kiecker, C., Lumsden, A., 2004. Hedgehog signaling from the ZLI regulates diencephalic regional identity. Nat. Neurosci. 7, 1242–1249.
Kiecker, C., Lumsden, A., 2005. Compartments and their boundaries in vertebrate brain development. Nat. Rev. Neurosci. 6, 553–564.
Kiecker, C., Lumsden, A., 2012. The role of organizers in patterning the nervous system. Annu. Rev. Neurosci. 35, 347–367.
Kobayashi, D., Kobayashi, M., Matsumoto, K., Ogura, T., Nakafuku, M., Shimamura, K., 2002. Early subdivisions in the neural plate define distinct competence for inductive signals. Development 129, 83–93.
Kolm, P.J., Sive, H.L., 1995. Efficient hormone-inducible protein function in *Xenopus laevis*. Dev. Biol. 171, 267–272.
Larsen, C.W., Zeltser, L.M., Lumsden, A., 2001. Boundary formation and compartition in the avian diencephalon. J. Neurosci. 21, 4699–4711.
Lowe, C.J., Wu, M., Salic, A., Evans, L., Lander, E., Stange-Thomann, N., Gruber, C.E., Gerhart, J., Kirschner, M., 2003. Anteroposterior patterning in hemichordates and the origins of the chordate nervous system. Cell 113, 853–865.
Martinez, S., Puelles, L., 2000. Neurogenetic Compartments of the Mouse Diencephalon and Some Characteristic Gene Expression Patterns. Results and Problems in Cell Differentiation, vol. 30, pp. 91–106.
Martinez-Ferre, A., Martinez, S., 2012. Molecular regionalization of the diencephalon. Front. Neurosci. 6, 73.
Martinez-Ferre, A., Navarro-Garberi, M., Bueno, C., Martinez, S., 2013. Wnt signal specifies the intrathalamic limit and its organizer properties by regulating Shh induction in the alar plate. J. Neurosci. 33, 3967–3980.
Mattes, B., Weber, S., Peres, J., Chen, Q., Davidson, G., Houart, C., Scholpp, S., 2012. Wnt3 and Wnt3a are required for induction of the mid-diencephalic organizer in the caudal forebrain. Neural Dev. 7, 12.
Moody, S.A., 1987. Fates of the blastomeres of the 16-cell stage Xenopus embryo. Dev. Biol. 119, 560–578.
Offner, N., Duval, N., Jamrich, M., Durand, B., 2005. The pro-apoptotic activity of a vertebrate Bar-like homeobox gene plays a key role in patterning the Xenopus neural plate by limiting the number of chordin- and shh-expressing cells. Development 132, 1807–1818.
Pani, A.M., Mullarkey, E.E., Aronowicz, J., Assimacopoulos, S., Grove, E.A., Lowe, C.J., 2012. Ancient deuterostome origins of vertebrate brain signalling centres. Nature 483, 289–294.
Pannese, M., Polo, C., Andreazzoli, M., Vignali, R., Kablar, B., Barsacchi, G., Boncinelli, E., 1995. The Xenopus homologue of Otx2 is a maternal homeobox gene that demarcates and specifies anterior body regions. Development 121, 707–720.
Peukert, D., Weber, S., Lumsden, A., Scholpp, S., 2011. Lhx2 and Lhx9 determine neuronal differentiation and compartition in the caudal forebrain by regulating Wnt signaling. PLoS Biol. 9, e1001218.
Puelles, E., 2007. Genetic control of basal midbrain development. J. Neurosci. Res. 85, 3530–3534.
Puelles, L., Rubenstein, J.L., 2003. Forebrain gene expression domains and the evolving prosomeric model. Trends Neurosci. 26, 469–476.
Redies, C., 2000. Cadherins in the central nervous system. Prog. Neurobiol. 61, 611–648.
Robertshaw, E., Matsumoto, K., Lumsden, A., Kiecker, C., 2013. Irx3 and Pax6 establish differential competence for Shh-mediated induction of GABAergic and glutamatergic neurons of the thalamus. Proc. Natl. Acad. Sci. USA 110, E3919–E3926.
Rodriguez-Seguel, E., Alarcon, P., Gomez-Skarmeta, J.L., 2009. The Xenopus Irx genes are essential for neural patterning and define the border between prethalamus and thalamus through mutual antagonism with the anterior repressors Fezf and Arx. Dev. Biol. 329, 258–268.
Sato, M., Kojima, T., Michiue, T., Saigo, K., 1999. Bar homeobox genes are latitudinal prepattern genes in the developing *Drosophila notum* whose expression is regulated by the concerted functions of decapentaplegic and wingless. Development 126, 1457–1466.
Scholpp, S., Foucher, I., Staudt, N., Peukert, D., Lumsden, A., Houart, C., 2007. Otx1l, Otx2 and Irx1b establish and position the ZLI in the diencephalon. Development 134, 3167–3176.
Scholpp, S., Lumsden, A., 2010. Building a bridal chamber: development of the thalamus. Trends Neurosci. 33, 373–380.
Scholpp, S., Wolf, O., Brand, M., Lumsden, A., 2006. Hedgehog signalling from the zona limitans intrathalamica orchestrates patterning of the zebrafish diencephalon. Development 133, 855–864.
Shimamura, K., Hartigan, D.J., Martinez, S., Puelles, L., Rubenstein, J.L., 1995. Longitudinal organization of the anterior neural plate and neural tube. Development 121, 3923–3933.
Turner, D.L., Weintraub, H., 1994. Expression of achaete-scute homolog 3 in Xenopus embryos converts ectodermal cells to a neural fate. Genes Dev. 8, 1434–1447.
Viczian, A.S., Zuber, M.E., 2010. Tissue determination using the animal cap transplant (ACT) assay in Xenopus laevis. J. Vis. Exp..
Vieira, C., Garda, A.L., Shimamura, K., Martinez, S., 2005. Thalamic development induced by Shh in the chick embryo. Dev. Biol. 284, 351–363.
Vieira, C., Martinez, S., 2006. Sonic hedgehog from the basal plate and the zona limitans intrathalamica exhibits differential activity on diencephalic molecular regionalization and nuclear structure. Neuroscience 143, 129–140.
Wilson, S.W., Houart, C., 2004. Early steps in the development of the forebrain. Dev. Cell 6, 167–181.
Zeltser, L.M., 2005. Shh-dependent formation of the ZLI is opposed by signals from the dorsal diencephalon. Development 132, 2023–2033.
Zeltser, L.M., Larsen, C.W., Lumsden, A., 2001. A new developmental compartment in the forebrain regulated by Lunatic fringe. Nat. Neurosci. 4, 683–684.